

# Single Molecule Tools to Investigate Terminal Deoxynucleotidyl Transferase (TdT) Mechanisms

Tommy Nguyen

August 08, 2019

## 1 Abstract

Unlike DNA polymerase, the enzyme Terminal Deoxynucleotidyl Transferase (TdT) has the unique ability to elongate single stranded DNA (ssDNA) without a template. Because of this, TdT has potential uses in applications ranging from basic laboratory experiments needing ssDNA to gene editing. However, whether TdT elongates ssDNA via a distributive diffusion or processive run process has not been studied. Therefore, this study aims to investigate the diffusion (D) of TdT using two single molecule tools: fluorescence correlation microscopy (FCS) with a custom-built confocal microscope and an anti-brownian electrokinetic trap (ABEL-Trap).

## 2 Introduction

Terminal Deoxynucleotidyl Transferase (TdT) is an enzyme unique in its ability to elongate ssDNA without a template.<sup>1</sup> TdT can elongate ssDNA using all four dNTPs at different rates.<sup>1</sup> The structure of TdT is almost exactly the same as DNA polymerase except for a loop that is assumed to prevent TdT from binding to a complementary strand.<sup>1</sup> TdT requires the ssDNA primer it is elongating to have a free 3' OH group and TdT only elongates at the free 3' end of ssDNA.<sup>1</sup> Additionally, the presence of divalent metal ions is needed for TdT to perform its function such as Cobalt or Magnesium.<sup>1</sup> Some studies have suggested that TdT requires the ssDNA primer to have at least 3 base pairs (bp) so it can bind.<sup>1</sup> New work has shown however that TdT can synthesize ssDNA de novo.<sup>2&3</sup> All of these conclusions were taken using bulk reactions, but some important questions still remain unanswered. How fast does TdT add nucleotides to a primer? What is the average run length of TdT? And when it unbinds the primer, how long does it take to find a new primer? Does TdT undergo a conformational change upon binding the nucleotide or primer? Does TdT use a distributive or processive process to elongate ssDNA? These questions cannot be measured using standard bulk reactions due to their nature which gives us the motivation to find these answers using single molecule methods. Additionally, by finding the answers to these questions, more knowledge about the function of TdT can be probed and potentially be taken advantage of for creating arbitrary sequences of ssDNA.

Most experiments today use bulk ensemble measurements to do experiments. For example, one can measure the average size of molecules with gel electrophoresis, or biochemical properties with chemical assays. While overall parameters can be measured this way, these forms of measurement don't have high enough resolution to record characteristics on the single molecule level. The transition states as an enzyme performs its function cannot be looked at or certain folding mechanisms during an intramolecular process. Only by analyzing one molecule at a time can these important characteristics be recorded. Therefore, in this study, we build a single molecule tool, a confocal microscope, to probe single molecule diffusion characteristics using FCS.

FCS is used to measure the diffusion characteristics of fluorescent molecules by looking at the average dwell time of the molecule in the confocal volume of our laser. Autocorrelation measures the self-similarity of a signal and most importantly, the time for the autocorrelation to decay to half of its max value is about the same as the duration of the signal. This will allow the measurement of dwell times from the autocorrelation function. The normalized autocorrelation function  $G(\tau)$  that is used to fit the measured photon count data is given by:

$$G(\tau) = \frac{\sum_t I(t)I(t - \tau)}{(\sum_t I(t))^2} - 1$$

where  $\tau$  is some time lag and  $I(t)$  is the signal at some time  $t$ .<sup>4</sup> This can be fitted for a model of the autocorrelation of a single diffusive species with the approximation that the confocal volume is a 3D gaussian:

$$G(\tau) = G(0)\left(1 + \frac{\tau}{t_D}\right)^{-1}\left(1 + \frac{\tau}{k^2 t_D}\right)^{-1/2}$$

where  $k = w_{xy}/w_z$ ,  $G(0)$  is the amplitude, and  $t_D$  is the diffusion time represented by  $t_D = \frac{w_{xy}^2}{4D}$  where  $D$  is the diffusion coefficient.<sup>4</sup> By fitting the model to the measured autocorrelation of a fluorescent molecule, the diffusion time can be extracted, and accordingly the diffusion coefficient given the size of our confocal volume. One disadvantage of using FCS is that the observation time is diffusion limited, typically 1ms. However, for this study of TdT, this is not a problem as the  $k_{cat}$  value of TdT as it elongates  $d(A)_{10}$  ssDNA using dATP gives:  $k_{cat} = 147/\text{min}$  or  $k_{cat} = 0.33 \text{ sec/reaction}$ , indicating that we should be able to see TdT bound to ssDNA using FCS.<sup>5</sup>

Lastly, time permitting, the elongation kinetics of TdT will be examined using an ABEL-Trap. The ABEL-Trap is an improved version of the built confocal microscope by trapping molecules in solution using feedback electric forces allowing extended observation of molecules on the order of 1-10 seconds. More specifically, the question of whether TdT undergoes distributive or processive elongation of ssDNA will be examined using the ABEL-Trap.

### 3 Materials and Methods

A diagram of the confocal set-up is shown below. The set-up is designed for both confocal and widefield microscopy:

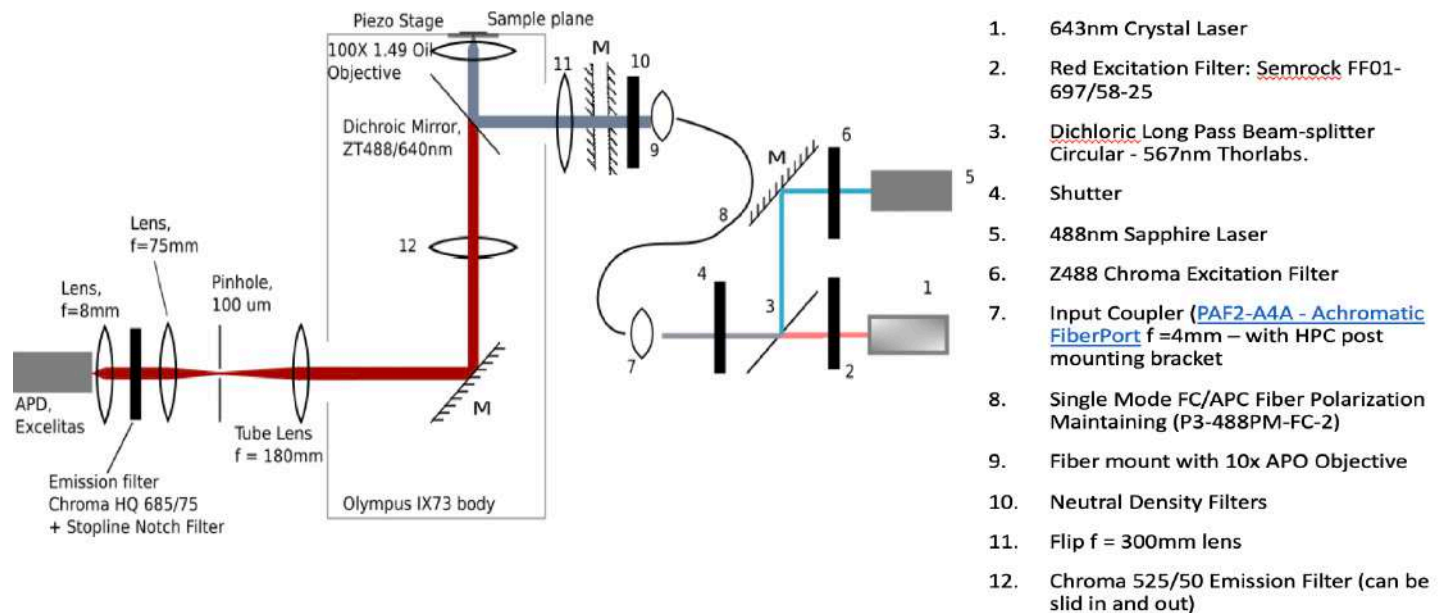


**Diagram 1: Diagram of the built set-up combining FCS and widefield microscopy.** 49mW 643nm crystal laser and 22.5mW 488nm Sapphire laser were used. A fiber was used to guide the beam path for flexibility in mounting. All optics are mounted on an optical table. Parts 1-7 are mounted on a raised optical bench. The objective is an Olympus UAPON 100x TIRF oil objective. The M's in the diagram correspond to mirrors for alignment of the beam. A black box covers the optics after the beam exits the microscope and black foil is used to enclose the detection area of the APD to decrease background.

The 643nm crystal laser and 488nm laser were chosen due to availability and their main uses in confocal and widefield microscopy respectively. Both lasers were mounted in such a way to allow space for addition of more lasers in case of wanting to do single molecule fluorescence resonance energy transfer (smFRET) measurements. An achromatic fiberport from Thorlabs was used to couple the lasers beams into the fiber. A built fiber output coupler was used consisting of a fiber mount with a 10x APO objective from Thorlabs. Taking

measurements of the beam power before and after fiber coupling gives coupling efficiencies of 38.22% for the 488nm laser and 37.1% for the 643nm laser. These were the maximum coupling efficiencies that could be achieved due to optical losses in the fiber. The polarization before and after coupling into the fiber was also checked and found to be relatively maintained for both lasers with extinction ratio percent differences of ~20% (Sup. Fig. 1). This is expected because a polarization maintaining fiber was used. Taking measurements of the beam profile after fiber coupling also shows that the lasers are approximately collimated (Sup. Fig. 2). The 488nm laser maintains its symmetric beam profile through a distance of 20m with slight elongation due to gaussian beam divergence. The 643nm laser maintains its beam profile through a distance of 6.5m as expected from an ideal gaussian beam whose width  $w(z)$  elongates as:

$$w(z) = w_0 \left[ 1 + \left( \frac{\lambda z}{\pi w_0^2} \right)^2 \right]^{\frac{1}{2}}$$

where  $w_0$  is the measured beam radius directly out of the coupler,  $\lambda$  is the beam's wavelength and  $z$  is the distance from the coupler (1). The decrease in the actual beam size at a distance of 20m from the fiber coupler suggests that the beam measured directly out of the fiber is not indicative of the true beam's smallest focus plane. Although this is the case, the 643nm beam can still be used as will be shown when using the confocal set-up for FCS. Another thing to note is that the beam coming out of the fiber coupler from the two lasers are different in size. The ratio of the produced beam sizes is approximately equal to the ratio between the two wavelengths which is expected since the mode diameter of the beam through the fiber is wavelength dependent. Right before entering the microscope, a 300mm focal length flip lens was added to allow the transition between confocal and widefield microscopy. When the lens is aligned with the beam, the set-up is in "widefield mode" due to the flip lens enlarging the illumination area, and when it is flipped out, the set-up is in "confocal mode" due to the laser spot being diffraction limited. In widefield mode, the illumination area's radius was measured to be ~0.32um (Fig. 1 Left). This is measured as the  $1/e^2$  radius by summing photon counts along each row in the image and fitting a gaussian. A piezo stage was added for micrometer precision in aligning the laser spot to measure the confocal volume used in FCS. At the sample plane,  $170 \pm 5$ um thick  $N_2$  gas and plasma cleaned glass coverslips were used in both microscopies for all samples. The Chroma 525/50 emission filter is placed into the beam path for widefield microscopy of Atto 488 dye and taken out for confocal microscopy.

The beam coming out of the microscope from the sample (detection path) is used for confocal microscopy. A 100um diameter pinhole is used to reject out of focus light coming from background and the sample. A transmission of 81.85% was achieved (Sup. Fig. 3). A black box enclosing the set-up and black foil covering the avalanche photodiode (APD) is used to generate photon counts similar to when a black cap is put on the APD (Sup. Fig. 5). To measure the confocal volume, a program in labview was modified to record the  $xy$  and  $xz$  dimensions of the point spread function of the laser (Sup. Fig. 5). The beam closely resembles a 3D gaussian with slight elongation in the  $x$  direction as expected from the linear polarization of our laser beam.<sup>6</sup> The confocal volume was measured to be  $3.568 \times 10^{-19} m^3$  with the  $xy$  dimension being 0.3193um, and the  $xz$  dimension being 0.8356um giving evidence of a diffraction limited spot for our laser (Sup. Fig. 5).

To do FCS measurements, 25uL of the given sample is pipetted into a chamber stuck with adhesive onto a glass cover slip. Before making measurements, unless otherwise noted, the focus spot of the laser is projected onto the glass-solution interface using a camera and then moved 15um into the sample to avoid having the confocal volume too close to the glass-solution interface. All autocorrelations were fitted with a simple diffusive model given above unless otherwise noted.

All gels shown in this report are Novex 15% TBE-UREA-PAGE precast gels from Invitrogen ran at 180V, 17mA, for 1 hour and 10 minutes. 15 well gels were used. Novex TBE-UREA sample buffer was used to load the samples.

## 4 Results and Discussion

### Widefield Results

With the 300mm flip lens and chroma 525/50 emission filter in the beam path, the performance of our built widefield microscope was tested using Atto 488nm dye molecules spin coated onto the glass cover slide. Looking at Fig. 1 Right, it can be seen that our widefield microscope works by being able to visualize single molecules as little dots in the image. This means nanometer sized molecules can be seen with our set-up!

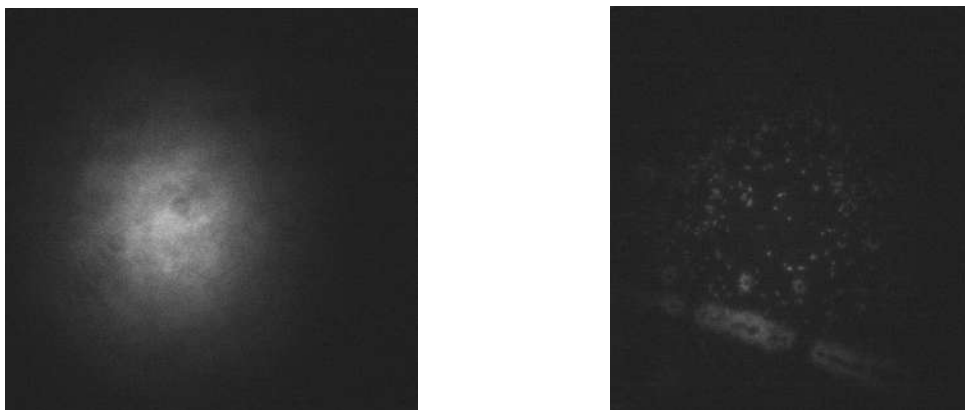


**Figure 1. Images of single Atto 488nm dye molecules using Widefield microscopy.** (Left) Picture of a widefield illumination spot of a 5.4uM Atto 488nm dye solution measured to be  $\sim 0.32\mu\text{m}$  in radius with a camera. A shutter of 44.753ms, a gain of 46.595dB, and a frame rate of 22.278fps was used in taking the image. OD1. (Right) Picture using the same widefield spot of 5.4nM Atto 488 dye. Same settings and OD were used as the left picture.

A couple of observations were made that were not shown in the figure. These molecules can be seen with one's own eyes! It was qualitatively found that our eye's resolution is better than the camera's at visualizing single molecules after  $\sim 20\text{min}$  of dark adaption. The molecules were also found to photobleach out of the image in  $\sim 135$  seconds (3 frames) at OD1. This suggests using a larger illumination spot or to use anti-faders to increase the photobleaching time in future experiments.

### Confocal Results

To test our built confocal microscope, we recorded the photon counts and measured the autocorrelation of 15pM Atto633 dye in PBS solution using a laser power of 7.9uW measured at the back aperture of the objective. A depth of 2um, instead of 15um was used.

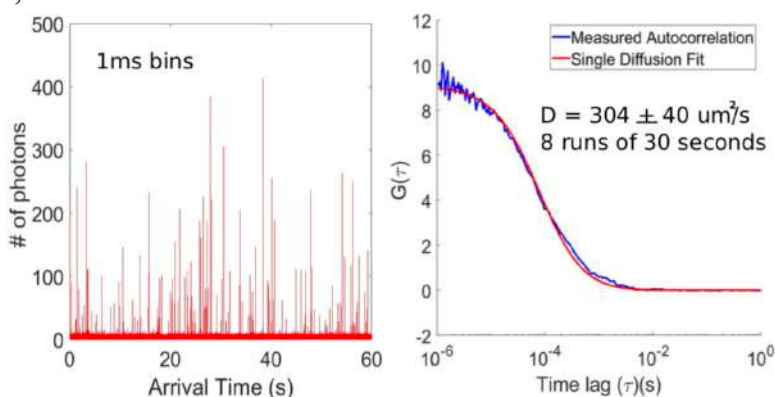


**Figure 2. FCS measurements of 15pM Atto633 dye using confocal microscopy.** (Left) The raw photon counts binned in 1ms time bins. (Right) Autocorrelation of the photon counts of the left plot. A diffusion coefficient of  $304 \pm 40\mu\text{m}^2/\text{s}$  was recorded using 8 runs of 30 seconds.  $\pm$  represents  $\pm 1$  standard deviation from the mean.

The typical diffusion coefficient of a fluorescent dye is around  $\sim 300\text{-}400\mu\text{m}^2/\text{s}$  indicating that our built confocal microscope works. The concentration limits for our confocal microscope were also tested by varying the concentration of Atto633 dye and observing the autocorrelation curve:

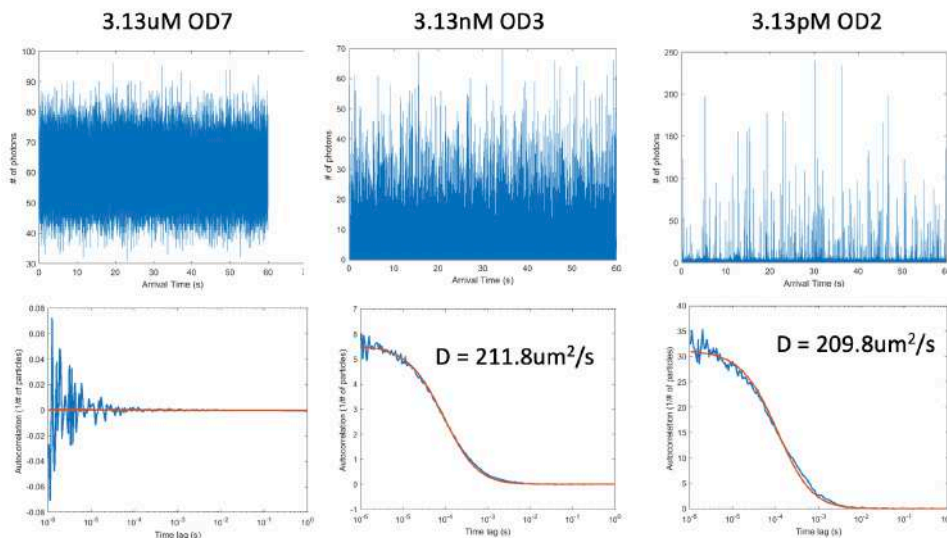


**Figure 3. FCS measurements of different concentrations of Atto633 dye.** (Top row) Raw photon counts for each concentration taken using 1ms time bins. (Bottom row) Measured and fitted autocorrelation curves. 60 seconds of data was recorded in 1ms bins.

Looking at Fig. 3, we can see that nM and pM concentration give relatively nice autocorrelation curves with a clear decay indicating that these concentrations of a fluorescence species can be measured using FCS. For the uM concentration, it can be seen that there is no noticeable curve. This might be because of the extremely high concentration saturating the confocal volume leading to fluctuations in the laser being more apparent than the diffusion fluctuations as molecules diffuse through the confocal volume. This would explain the low amplitude seen in the bottom left figure at uM concentration. Nonetheless, uM concentrations cannot be recorded with our confocal set-up.

The diffusion coefficient measured in Fig. 3 is relatively low compared what is measured in Fig. 2. It was believed that this is due to taking measurements at different depths from the glass-solution interface. We tested this hypothesis by measuring the diffusion coefficient at different depths of .313nM Atto633 dye. Our results are given below:

Depth ( $\mu\text{m}$ ) *All taken at OD3	# of Trials	Diffusion Coefficient ( $\mu\text{m}^2/\text{s}$ )	Amplitude (1/# of molecules)	Calculated Concentration (nM)
+0	8	$308.3 \pm 23.07$	$16.3 \pm .41$	.285
+1	8	$317.8 \pm 10.1$	$16.6 \pm 0.51$	.280
+2	8	$327.2 \pm 8.03$	$14.5 \pm 0.23$	.321
+3	8	$301.1 \pm 10.32$	$12.4 \pm 0.14$	.375
+5	8	$287.1 \pm 4.37$	$10.4 \pm 0.20$	.448
+10	8	$266.4 \pm 7.78$	$7.7 \pm 0.16$	.606
+15	8	$256.2 \pm 4.739$	$6.0 \pm 0.36$	.774

**Figure 4. FCS measurements of Atto633 dye taken at different depths from the glass-solution interface.** All  $\pm$  are standard deviations from the mean of 8 trials w/ 30 sec runs of 1ms bins.

Looking at Fig. 4, it can be seen that as the depth increases, the diffusion coefficient decreases. This is an interesting phenomenon and explains our lower diffusion coefficient at a depth of 15um in Fig. 3 compared to a depth of 2um in Fig. 2. As to the reason on why this relationship is present, more studies need to be conducted, but we currently believe that the model of the confocal volume doesn't consider refraction at the glass-solution interface. This refraction might cause unaccounted effects on the 3D gaussian assumption of the confocal volume.<sup>6</sup> Future experiments investigating the true point spread function at different depths would be interesting to study and would allow the determination of what the diffusion coefficient actually is at different depths.

## TdT Results

Now that the built confocal microscope is proven to be functional, TdT can now be investigated using FCS. However, whether TdT can elongate fluorescently labeled ssDNA needs to be answered. To answer this question, a UREA-PAGE gel was ran:



**Figure 5: Photo of a UREA-PAGE gel ran investigating whether TdT can elongate 5' fluorescently labeled ssDNA strands.** The reaction consisted of: 10 pmol ssDNA, 82nM TdT, 100uM dCTP, 250 CoCl<sub>2</sub> with 10X TdT buffer (from Invitrogen) incubated at 37°C for 30min.

Looking at the bands in Fig. 5, one can see that all strands, whether or not they were 5' modified, were able to be elongated by TdT. This proves that TdT can elongate 5' modified strands and is ready to be investigated with FCS.

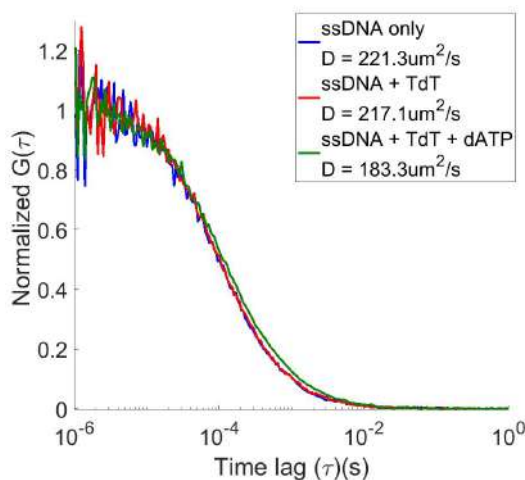


**Figure 6. FCS of ssDNA and ssDNA elongated by TdT.** A reaction mixture containing: 1.25nM of ssDNA (2 strand from Fig. 5), 82nM TdT, 250uM MgCl<sub>2</sub>, 100uM dATP, in PBS buffer incubated at 37°C for 5 minutes. Measured at a depth of 2um from the glass-PBS interface with a laser power of 79nW at the back aperture of the objective.

The first thing that was measured was whether TdT elongated ssDNA strands could be looked at. Looking at Fig. 6, a diffusion coefficient of  $221.3\mu\text{m}^2/\text{s}$  was recorded with only ssDNA. By adding TdT and dATP, the diffusion coefficient changed to  $183.3\mu\text{m}^2/\text{s}$  giving a slower diffusion. This indicates that TdT elongated the ssDNA strand and this elongation was able to be recorded using FCS. An interesting thing to note from Fig. 6 is that ssDNA + TdT didn't give a noticeable change in  $D$  compared to only ssDNA. One would expect a lower  $D$  because of the potential measurement of the ssDNA bound to TdT complex. The reason for why this isn't observed may be because of the relative concentration of ssDNA to TdT. To see if this was really the case, the concentration of TdT was increased in proportion to ssDNA and whether or not TdT bound to ssDNA was investigated using FCS:

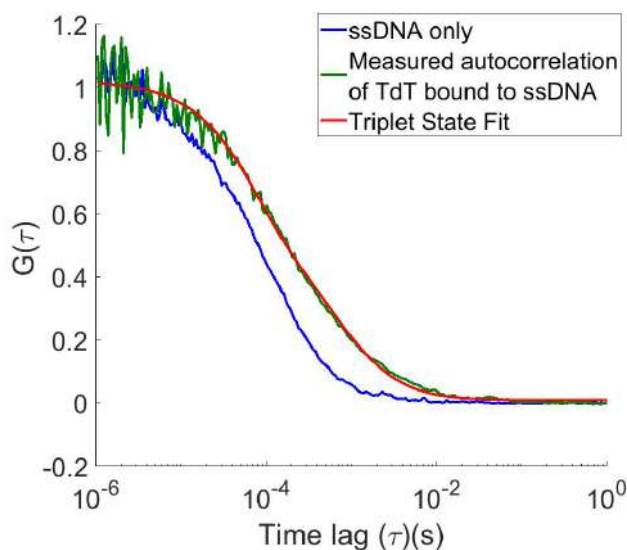


**Figure 7. FCS of ssDNA and ssDNA bound to TdT.** A reaction mixture containing: 1.25nM of ssDNA (2 strand from Fig. 5), 820nM TdT, 330uM  $\text{MgCl}_2$ , 1X TdT buffer in  $\text{H}_2\text{O}$  was used. Measured at a depth of 15um from the glass-solution interface with a laser power of 79nW at the back aperture of the objective. A triplet state fit was fitted to the TdT bound to ssDNA due to the triplet characteristics of the fluorophore Cy5 attached to the ssDNA. A  $D = 50.44 \pm 7.83 \mu\text{m}^2/\text{s}$  was extracted from the fit from 8 runs of 30 seconds each. The  $\pm$  represents  $\pm 1$  standard deviation from the mean.

Looking at Fig. 8, it can be seen that the diffusion of TdT with ssDNA is slower than only ssDNA. A diffusion coefficient of  $50.44\mu\text{m}^2/\text{s}$  was measured of TdT with ssDNA giving strong evidence that TdT bound to ssDNA is being measured.

## 5 Conclusion

In summary, FCS using our custom-built confocal microscope can be used to measure the diffusion of TdT as it is bound to ssDNA and whether or not ssDNA has been elongated by TdT. This gives rise to further investigations using FCS and the ABEL-Trap to look at more specific unanswered questions about TdT, such as: whether or not TdT elongates ssDNA via a distributive or processive process, the relationship between metal ions and base elongation rate, and whether the diffusion coefficient of denovo synthesized ssDNA using TdT is similar to regular ssDNA. These future experiments will further our understanding of the kinetics of TdT which can later be used to easily synthesize ssDNA.

## 6 Acknowledgments

*This paper represents my own work in accordance with University regulations – Tommy Nguyen.* I'd like to thank Quan Wang and Hugh Wilson for help with the experiments and design, and the Wang Lab for ideas and discussion.

## 7 References

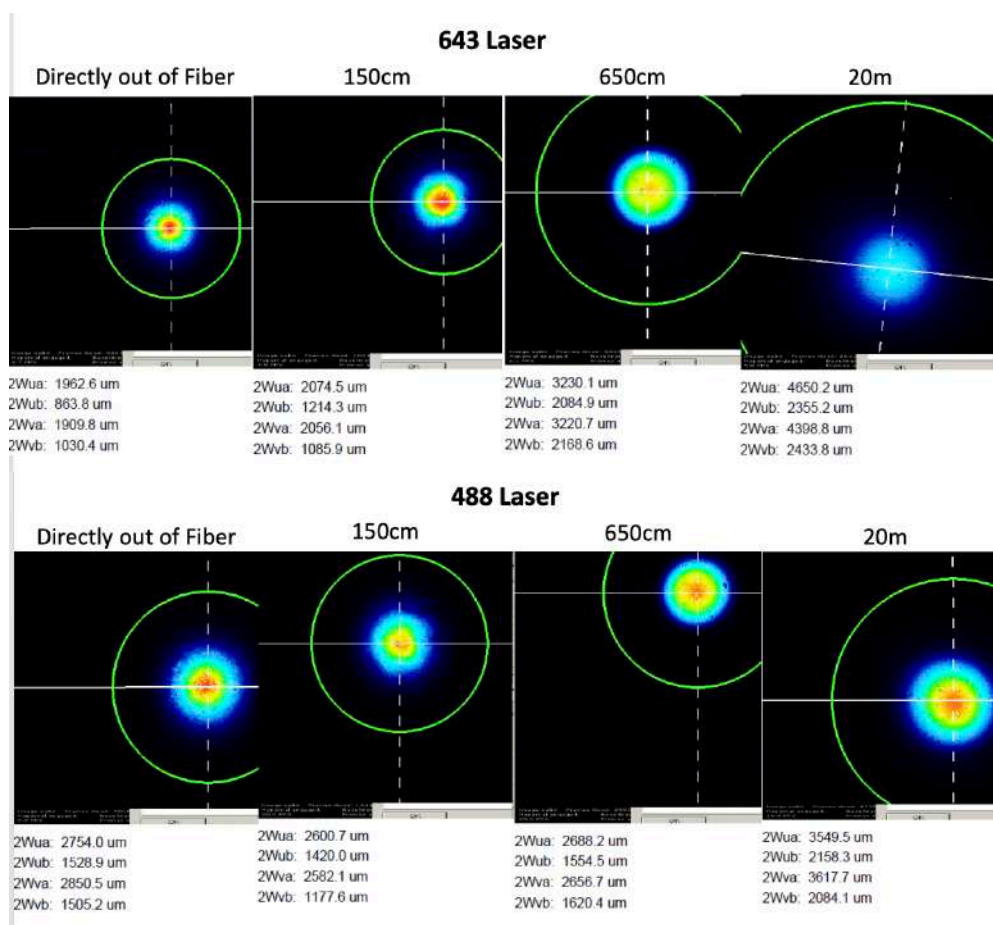
- [1] Motea, E. A., & Berdis, A. J. (2010). Terminal deoxynucleotidyl transferase: the story of a misguided DNA polymerase. *Biochimica et biophysica acta*, 1804(5), 1151–1166. doi:10.1016/j.bbapap.2009.06.030
- [2] Palluk, S., Arlow, D. H., De Rond, T., Barthel, S., Kang, J. S., Bector, R., ... Keasling, J. D. (2018). De novo DNA synthesis using polymerasenucleotide conjugates. *Nature Biotechnology*, 36(7), 645–650. <https://doi.org/10.1038/nbt.4173>
- [3] Ramadan, K., Shevelev, I., Maga, G., & Hubscher, U. (2004, April 13). De Novo DNA Synthesis by Human DNA Polymerase  $\lambda$ , DNA Polymerase  $\mu$  and Terminal Deoxyribonucleotidyl Transferase. Retrieved August 6, 2019, from <https://www.sciencedirect.com/science/article/pii/S0022283604003705?via=ihub>
- [4] Buschmann, V., Krämer, B., Koberling, F., Macdonald, R., & Rüttinge, S. (2007). Quantitative FCS: Determination of the Confocal Volume by FCS and Bead Scanning with the MicroTime 200. *AppNote Quantitative FCS*, 1–8.
- [5] Boulé, J.-B., Rougeon, F., & Papanicolaou, C. Terminal Deoxynucleotidyl Transferase Indiscriminately Incorporates Ribonucleotides and Deoxyribonucleotides. Retrieved from <http://www.jbc.org/content/276/33/31388.full.pdf.html>
- [6] Michael J. Nasse and Jörg C. Woehl, "Realistic modeling of the illumination point spread function in confocal scanning optical microscopy," *J. Opt. Soc. Am. A* 27, 295-302 (2010)



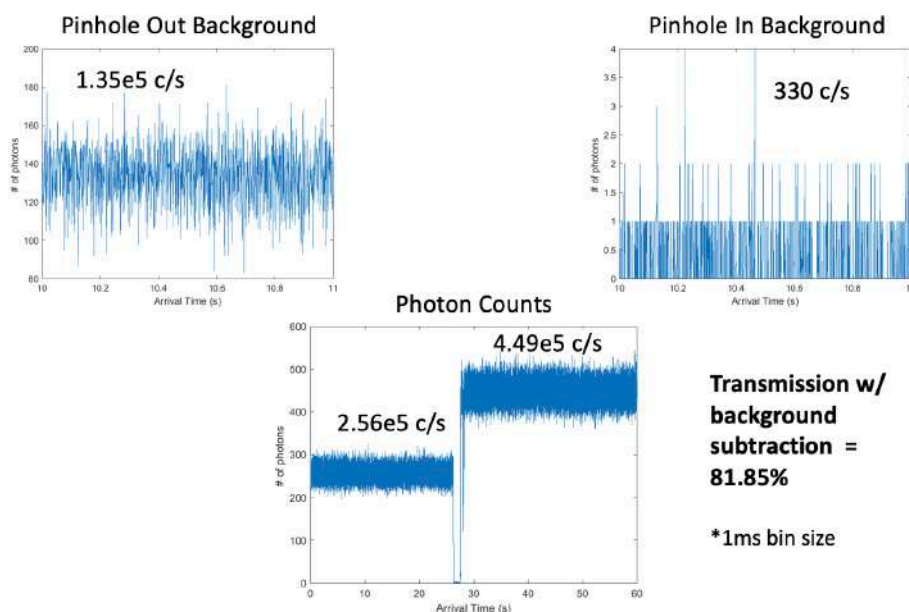
## 8 Supplementary Information

	488nm Laser	643nm Laser
Extinction Ratio Right Before Fiber	1075.6 (30.32 dB)	91.34 (19.6 dB)
Minimum Power w/ standard deviation	0.01362 ± 0.0001 mW	0.464 ± 0.002 mW
Extinction Ratio After Fiber	1240 ± 190 (30.93 dB)	70.2 ± 28 (18.46 dB)
Minimum Power w/ standard deviation	0.0065 ± 0.001 mW	0.25 ± 0.1 mW
Extinction Ratio Percent Difference	14.2%	26.17%

Supplementary Figure 1. Measurements of the extinction ratio before and after fiber coupling for both lasers.



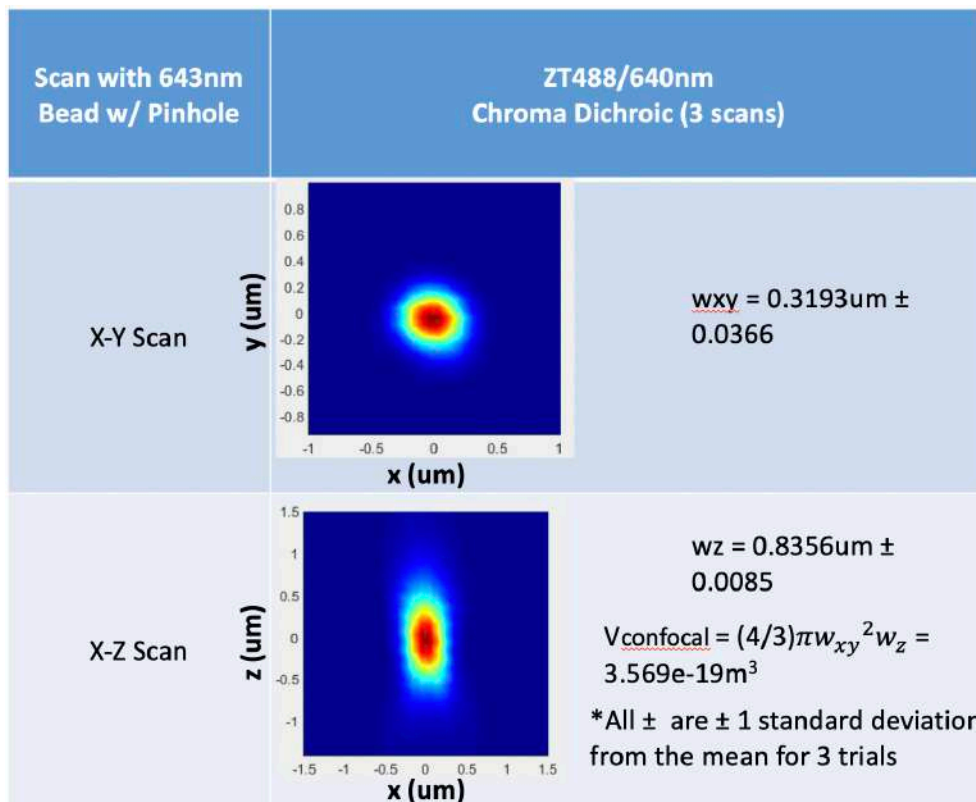
Supplementary Figure 2. Measurements of the beam profile at various distances from the fiber coupler of both lasers.



**Supplementary Figure 3. Photon counts of the background and of a 643nm fluorescent bead with and without the pinhole.**

Characterizations	Mean # of Photons/Second
Dark Count w/ cap (front)	90.21 ± 1.23
Dark Count w/ cap (back)	89.79 ± 1.22
Background Count with no cap	1.9863*10 <sup>5</sup> ± 57.54
Tent with Front Monitor on	1004.5 ± 4.09
Tent with Back Monitor on	113 ± 1.37
Black Foil no tent (front)	6400 ± 10.33
Black Foil w/ tent (front)	91.13 ± 1.23
Black Foil no tent (back)	168.46 ± 1.68
Black Foil w/ tent (back)	89.34 ± 1.22

**Supplementary Figure 4. Photon counts characterizing the efficiency of the black box and foil surrounding the detection path.** ± represents ±1 standard deviation from the mean for 60 trials of 1ms bins. The front and back tags represent a front monitor close to the set-up being on and a back monitor on with the front off respectively.



**Supplementary Figure 5. Bead scans characterizing the confocal volume of the microscope.** 643nm beads were spin coated on coverslips as samples. Dwell time of 20ms and a scan range of 2 $\mu\text{m}$  for xy and 3 $\mu\text{m}$  for xz were used. 30 points were taken for both xy and xz.